

A new cement slurry modified with chitosan/alginate interpenetrating networks and hydroxyapatite – structural characteristics after long-term contact with hyper-saline produced water from oil well operations

Ivory Marcos Gomes dos Santos¹, Danilo Oliveira Santos¹,
Antonio Reinaldo Cestari¹, Joenesson Filip Santos Ribeiro²,
José do Patrocínio Hora Alves³, Angélica Baganha Ferreira³

¹ Department of Materials Science, Federal University of Sergipe, CEP 49100-000, São Cristóvão, Sergipe, Brazil.

e-mail: ivorymarcos@hotmail.com; danilo.quimico@yahoo.com.br; arcestari@gmail.com

² Laboratory of Materials and Calorimetry, Department of Chemistry/CCET, Federal University of Sergipe, CEP 49100-000, São Cristóvão, Sergipe, Brazil.

e-mail: joenesson.joe@hotmail.com

³ Technological and Research Institute of the State of Sergipe, CEP 49020-380, Aracaju, Sergipe, Brazil.

e-mail: jphalves@uol.com.br; angelica.bferreira@itps.se.gov.br

ABSTRACT

Oil is an important source of energy, mainly in developing countries. Important research has been conducted to find cementing procedures that guarantee safe and cost-effective oil exploration below pre-salt layers. This work aimed to make a new cement paste with cement, seawater, silica, biopolymers (chitosan and sodium alginate) and hydroxyapatite (HA), found in nature. For comparison purposes, slurry without additives was prepared and characterized. The HA used was extracted from fish scales (*Cynoscion acoupa*) in optimized condition NaOH concentration, temperature and reaction time. Both slurries were prepared with ratios water/cement (w/c) and silica/cement (s/c) equal to 0.50 and 0.35, respectively. The new cement slurry was obtained with proportions of 5% of each biopolymer and HA with respect to the total weight of the cement. In the immersion tests, specimens were immersed in samples of hyper production of saline water by 35°C for 15 days. Thereafter, they were washed, dried and its surface layers were scraped. Before, the resulting materials were characterized. The values of the ratios Ca/Si of new cement slurry (3.38 ± 0.06) were superior compared to standard (2.58 ± 0.05). The new slurry had high thermal stability and low amounts of small crystallite-type portlandite (35.70 nm). Conversely, a slurry standard formed larger crystals of about 50.3 nm. Significantly, after continuous long-term contact of both slurries with hyper-saline produced water from oil well fields operations, in comparison with standard slurry structural characteristics, the new slurry has practically maintained its pristine chemical structure, as well as has shown crystallite-type particles of NaCl and Friedel's/Kuzel's salts with lower proportion. The presence of the biopolymers and HA has driven the improved the self-healing properties observed in the new cement slurry. In this first study, the new slurry has shown adequate characteristics to contribute to cost effective and environmental-friendly oil well operations.

Keywords: Cement slurries, biopolymers, hydroxyapatite.

1. INTRODUCTION

Oil is still an important source of energy, mainly in developing countries, with demands ranging up to about 65 million oil barrels per day in a near future. Driven by such needs, oil and natural gas were recently found to lie below a 2,000-3,000 meter deep saline geological formation of the coast of South America and Africa (the pre-salt region), formed in remote ages due to evaporation of seawater [1]. However, most of oil below pre-salt layers has not leaked properly, because drilling through rocks to extract the pre-salt oil is very expensive and dangerous. Indeed, undersurface salts are typically plastic and mobile, and they produce undesirable shifts in overburden pressure over time and wells collapses [2]. Significant research efforts are therefore being spent on new cementing procedures to provide safe and cost-effective oil exploration below pre-salt layers.

Appropriate water-based cement slurries have been used to provide both a reliable isolation to prevent undesirable migration of fluids between well zones and a good well integrity [3]. The quality of the water used to mix oil well cement is a very important parameter and varies depending upon the technical specifications of cementing procedures. Because of the growing offshore procedures, seawater has become very widely used for oil wells cementing [4]. On the other hand, oil and gas industries use large amounts of water-based compounds, which can solve specific underground problems. As a consequence, the so-called produced water is considered the largest water-based stream generated in oil and gas field.

Produced water is a mix of inorganic and organic compounds, and its characteristics depend on the nature of the chemicals used in well procedures and the operational conditions [5]. However, it is reported that cement slurry properties can be negatively affected by long-term contact with hyper-saline water-based media. It is therefore important to address the characteristics of long-term contact of oil well cement slurries with hyper-saline produced water to assure long-term structural stability of the hardened slurry to avoid zonal isolation of some parts of oil wells and environmental contamination problems [6]. Specific polymers have been used to improve some important characteristics of oil well slurries for cementing procedures.

Low amounts of water-soluble polymers have been used extensively in oil well cementing, mainly for partial completion and workover, with variable degrees of success [7]. Indeed, many polymeric systems employed in oil well cementing have not provided enough technological and economical characteristics to be used in routine operations in oil field. In this manner, polymers-incorporate cement-based materials with self-healing properties may be a useful and effective option to be used in this field [8].

Self-healing oil well cement systems typically are made of cement, water and specific swellable hydrophilic polymers, preventing diffusion of fluids into cement bodies. In addition, such polymeric networks can decrease or avoid the formation or precipitation of specific and undesirable compounds in the hardened slurry, which could weak the structural characteristics of the hardened cementitious body. Evidently, such self-healing performance strongly depends on the nature of the polymers in a given cement slurry [9]. In this sense, an alternative emerging approach is to utilize some naturally occurring polymers as low cost and effective self-healing materials for using in oil well cementing procedures, such as chitosan and alginic acid.

Chitosan is a polysaccharide consisting of D-glucosamine and N-acetyl-D-glucosamine units [10]. On the other hand, alginates possess polysaccharide backbones comprised of linear copolymers of (1-4)-linked β -D-mannuronate and residues of C-5 epimer α -L-guluronate, which are linked together in specific sequences [11]. Indeed, engineering interpenetrating polymeric networks of chitosan and alginates and can ionically interact each another to form cross-linked three-dimensional matrixes with outstanding properties. However, such polymeric networks are reported to present weak structural mechanical properties [10]. To try solve this problem, the inclusion of inorganic-type nano- or mesoparticles, such as hydroxyapatites, has been the main objective of improving the mechanical properties of chitosan/alginate polymeric matrixes [12]. Hydroxyapatite $[\text{Ca}_{10}(\text{PO}_4)_6(\text{OH})_2]$ constitutes the main inorganic matrix of bones and tooth tissues. Specifically, naturally occurring hydroxyapatite (HA), resulting from highly specific biological processes, often exhibits improved molecular-level characteristics in comparison with synthetic hydroxyapatites [13]. The unique properties of HA are believed to significantly improve the morphological characteristics of chitosan, via strong ionic interaction of protonated chitosan and anions from HA (mainly PO_4^{3-} groups) [13].

In this work, we report the preparation and structural characterization of a new cement slurry additived with chitosan/alginate/HA in seawater. HA was extracted from fish scales by a chemometrically optimized alkaline heat-treatment method. To the best of our knowledge, this is one of the very limited examples of the use of biopolymers and HA in cement slurries formulations. Additionally, the structural characteristics of the new slurry were presented and discussed, after long-term contact with a sample of hyper-saline produced water supplied from oil well procedures.

2. MATERIALS AND METHODS

2.1 Materials

Class A oil well cement and silica are of particles diameters of 200-325 and 325 mesh, respectively, were a free gift from Schlumberger - Petroleum Services Ltd. The chitosan powder (CS), with 80% of deacetylation degree, was a gift from C.E. Roeper, Germany. The sodium alginate (ALG) was utilized in powder form and acquired Cromoline Company. The seawater and the produced water samples were both sent to our research group by Petrobras - Petroleum Services (Brazil), from an oil well plant near city of Nossa Senhora do Socorro, Sergipe state, Brazil.

Fish (*Cynoscion acoupa*) scales were washed with water to remove dirty substances and dried at room temperature for 24 h. A preliminary 2³ full factorial design study was randomly carried out to find the best experimental condition to obtain collagen-free HA from raw fish scales, using an alkaline hydrolysis procedure of collagen-based materials [14]. The best results were obtained for raw fish scales in contact with 1.0 mol·L⁻¹ NaOH solution, heated up to 60°C under continuous stirring for 24 h.

2.2 Preparation of the cement slurries

The cements slurries were prepared as described earlier in literature [15, 16], targeting final densities of the slurries of about 1.75 ± 0.15 g/cm³ [4, 15]. The main slurry was prepared with 200 g of dry cement, 70 g of silica, 100 mL of seawater (w/c = 0.50 and s/c = 0.35), and a mixture of CS, ALG and HA. In order to not change the mandatory rheological characteristics of the slurry, the ratio of each component of the mixture was 5:5:5 (% in relation to cement mass) [17]. The cement gel obtained was mixed at 12,000 rpm for 15 s (pre-mixing of the wet and dried components) and 35 s for a enough mixing of all components of the wet slurry. The cement slurry was cast into 5.0 cm side cubic molds and stored in a desiccator saturated with the water vapor at room temperature for 6 h prior to removal from the molds. The cement bodies were then cured directly in seawater for 28 days at 25°C. A slurry with only cement, silica and water, as a control material, was prepared and hydrated using the same procedure. For simplicity, the cement slurries are hereafter denominated as slurry-standard (cement/silica) and slurry-pol (cement/silica/CS, ALG, HA).

2.3 Long-term immersion tests in hyper-saline produced water

The demoulded cement slurry was immersed in 100 mL of produced water in a continuous contact for 15 days in a sealed container maintained in a temperature-controlled bath at 35°C, which is the average temperature of contact of the main cemented bodies with hyper-saline produced waters in Brazilian oilfields [18]. The samples were then extensively washed with distilled water to remove inorganic or organic components precipitated on the surface of the specimens, until undetectable presence of the ions from produced water on the surface of the materials, which was verified by conductometric measurements [18]. After that, the samples were dried at 50°C for 12 h. Cement samples were carefully removed from the surface of the cemented specimens and characterized.

2.4 Characterization of the samples

Fourier transform infrared spectroscopy (FTIR) spectrometry (Shimadzu FT-IR System Spectrum Prestige-21) was employed to determine the characteristics of chemical groups in the cement slurries, at room temperature [16]. KBr pressed-disks technique was used in a spectral from 4000 to 900 cm⁻¹. Thermogravimetric analysis (TG/DTG) was made using about 10 mg of a given material, under nitrogen atmosphere from 25 to 1000°C, in a SDT 2960 thermoanalyzer, from TA Instruments. Differential scanning calorimetry (DSC) analysis were performed in sealed Al pans, using about 10 mg of a given material, under nitrogen atmosphere from 25 to 500°C. The X-ray diffraction (XRD) diffractograms of the cement samples were obtained in a Shimadzu LABX 6000 diffractometer, in the 2θ range from 5 to 60° (accumulation rate of 0.02° min⁻¹), using CuKα radiation (λ = 1.5401 Å).

The quantification of the main ions in the produced water sample was performed using a Thermo Scientific Dionex ICS-3000 Ion Chromatography, with automatic both sample dilution and partial loop injection of the diluted sample [18]. Average elemental concentration of the main chemical elements of the samples was measured at different locations within individual particles by energy-dispersive X-ray spectroscopy (EDX) using an SHIMADZU 720 X-ray fluorescence spectrophotometer and normalized to 100 wt%.

3. RESULTS AND DISCUSSION

3.1 Characterization of the produced water

Produced water has been described worldwide as a complex sample. The main inorganic components of the produced water are shown in Table 1. Indeed, the main components of produced waters are dissolved salts from inorganic components, exceeding those found in seawater. The values found in this study for inorganics in produced water are relatively similar to others described in literature. Heavy metals and organics were, however, found to be undetectable, because such components in Brazilian produced water samples are typically found to be in concentration averages lower than the detection limit of the analytical method (usually less than 0.1 mg·L⁻¹) [18].

Table 1: Concentration (mg/L) of the main inorganic ions in the water production.

ION CONCENTRATION (mg/L)									
Cl ⁻	Mg ²⁺	Na ⁺	Ca ²⁺	K ⁺	SO ₄ ²⁻	S ²⁻	F ⁻	NO ₃ ⁻	NO ₂ ⁻
93,280	19,730	7,079	4,979	888.6	85.8	20.3	1.81	0.02	0.01

3.2 Characterization of the main materials used for the preparation of cement pastes

In the EDX analysis of the main materials used for preparation of cement pastes, presented in Table 2, were identified and quantified various chemical elements characteristic of silica and class A portland cement.

Table 2: EDX analysis of the starting raw materials used for the preparation of cement pastes.

SAMPLE	ELEMENT (%)									
	Ca	Si	Fe	Al	S	Mg	K	Sr	Ti	Mn
Class A portland cement	74.63	12.24	5.57	3.15	1.86	1.09	0.67	0.33	0.23	0.11
Silica	ND	97.46	0.25	1.63	0.31	ND	ND	ND	0.16	ND

ND: Not detected.

The results of XRD analysis of the main materials used for preparation of cement pastes, in Figure 1, show that silica and class A portland cement are materials that exhibit high crystallinity, with well-defined crystallographic phases. The analysis of the diffractograms was made from data of Inorganic Crystal Structure Database (ICSD). For silica, the main peaks were identified in 2θ equal to 21.1, 26.8 and 50.3°. For class A portland cement, which is used to cement oil wells, the chemical composition are mainly found by silicate tricalcium, $3\text{CaO}\cdot\text{SiO}_2$ (C_3S , alite), silicate dicalcium, $2\text{CaO}\cdot\text{SiO}_2$ (C_2S , belite), tricalcium aluminate, $3\text{CaO}\cdot\text{Al}_2\text{O}_3$ (C_3A), and calcium aluminoferrites, $4\text{CaO}\cdot\text{Al}_2\text{O}_3\cdot\text{Fe}_2\text{O}_3$ (C_4AF), among others, for example calcium oxide (CaO) [4, 15]. In the Figure 1 (B), peaks were identified relating to C_3S ($2\theta = 29.4, 32.3^\circ$ and 56.4°), C_2S ($2\theta = 38.8$ and 41.4°), C_3A ($2\theta = 46.9^\circ$), C_4AF ($2\theta = 45.9^\circ$) and CaO ($2\theta = 34.4$ and 51.8°).

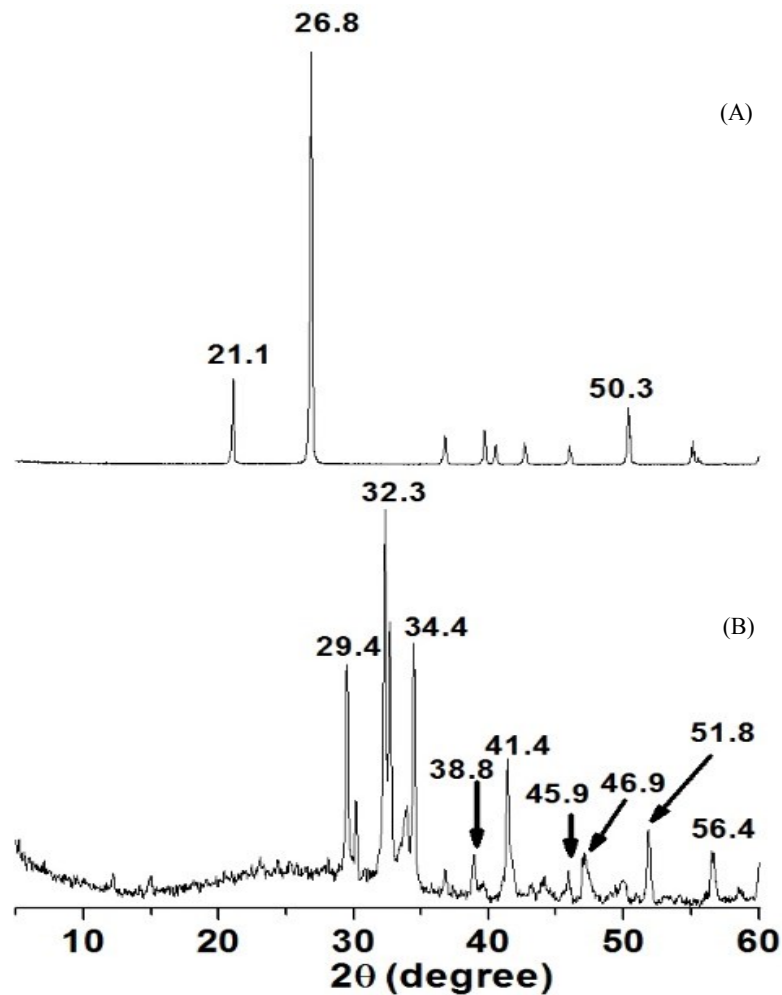


Figure 1: X-rays diffractograms of the starting raw materials used for the preparation of cement pastes. Silica (A) and class A portland cement (B).

3.3 Structural characterization of the cement samples

During the cements hydration reaction with water, alite and belite undergo dissolution reactions generating mainly calcium-silicate-hydrates (C-S-H), a monosulfate-type phase [$3\text{CaO} \cdot (\text{Al,Fe})_2\text{O}_3 \cdot \text{CaSO}_4 \cdot n\text{H}_2\text{O}$] (AFm phase), which is produced when C_3A reacts with CaSO_4 as well as calcium hydroxide (CH, portlandite). CaCO_3 is also produced due to secondary reactions between CH and C-S-H with CO_2 [4]. C-S-H is the main responsible for setting of the cement and strength development. Silica in combination with the other components of cement slurry improves mechanical properties to the compositions and producing low-porosity hardened slurries, which have the ability to properly withstand stresses found in subterranean conditions without significant formation of failures, crackings and occurrence of bond loss [19]. In this work, the cement slurries were prepared using seawater. The influence of seawater on the morphological characteristics of cement-based materials is rather complex due to the potentially aggressive ions present in such water medium such as carbonates, sulfates and chlorides [20].

Results from EDX analysis of the cement slurries are presented in Table 3. Measured atomic ratios are considered as an average chemical composition of the analyzed bulk of the material. In fact, the main hydrates in cement slurries contain Ca and are of particular interest. Some important qualitative structural characteristics of such hydrates have been found from the solid-state Ca/Si ratio of cement slurries [20, 21]. In the presence of low amounts of Ca^{2+} ions, the Ca/Si molar ratios in the interlayer space of C-S-H are typically less than unity, and the silicate chains are typically long and linear with compensation charges made by alkaline ions (Na^+ and/or K^+). For Ca/Si molar ratios of about 1.5, tetrahedral silicate sheets contain mainly dimers, and for Ca/Si ratios higher than 1.5, and CH may be in the interlayer space, with Al redistribution in the tetrahedral C-S-H sites and absence of Si^{4+} substitutions, leading to mainly formation of silicate chains constituted of dimers [21]. Indeed, the Ca/Si ratio measured in the cement slurries increased

with the presence of CS/ALG/HA additives. In the case of slurry-pol, the higher amount of Ca content in relation to slurry-standard one may be caused a redistribution of Al in the silicate chains in favor of specific bridging sites, where Al^{3+} preferentially substitutes a nonbridging Si^{4+} [20, 21].

Table 3: EDX analysis of slurry-standard and slurry-pol.

ELEMENT (%)	SLURRY-STANDARD	SLURRY-POL
Ca	63.30 ± 0.35	65.79 ± 0.31
Si	24.58 ± 0.30	19.44 ± 0.43
Fe	5.67 ± 0.11	5.28 ± 0.37
Al	2.39 ± 0.01	2.74 ± 0.30
S	2.50 ± 0.13	1.95 ± 0.04
P	ND	1.55 ± 0.01
Mg	1.02 ± 0.05	1.11 ± 0.01
Ti	0.26 ± 0.01	0.29 ± 0.01
K	0.21 ± 0.01	0.50 ± 0.15
Mn	0.07 ± 0.03	0.16 ± 0.01
Ca/Si (Ratio)	2.58 ± 0.05	3.38 ± 0.06

ND: Not detected.

The functional chemical groups of the cement slurries were evaluated using FTIR spectrometry and the results are shown in Figure 2. This technique provides qualitative information related to the presences of polymerized silicates, CH, condensed tetrahedra chains (TO_4), where T = Si or Al (Al-O-Si or Si-O-Si bonds), adsorbed water and compositional water, and carbonate polymorphs [22]. For the FTIR spectrum of slurry-standard, the bands with maximum at 3,697 and 3,450 cm^{-1} have been associated with the presence of CH and water bound in the hydration products, respectively. The bands centered at 1,445 cm^{-1} correspond to two elongation modes of C–O bonds of carbonates. The small band at 1,795 cm^{-1} is also associated the presence of C=O bonds from carbonates [23]. The bands from about 960 to 1,100 cm^{-1} are related to asymmetric Si-O stretching, out-of-plane and in-plane Si-O bending vibrations of SiO_2 quartz. Figure 2 shows the FTIR spectrum of slurry-standard after contact with the produced water. The absence of the band at about 3,700 cm^{-1} suggests the removal, at least partially, of CH. The main structural backbone characteristics of C-S-H of this slurry, however, seem not to be significantly affected.

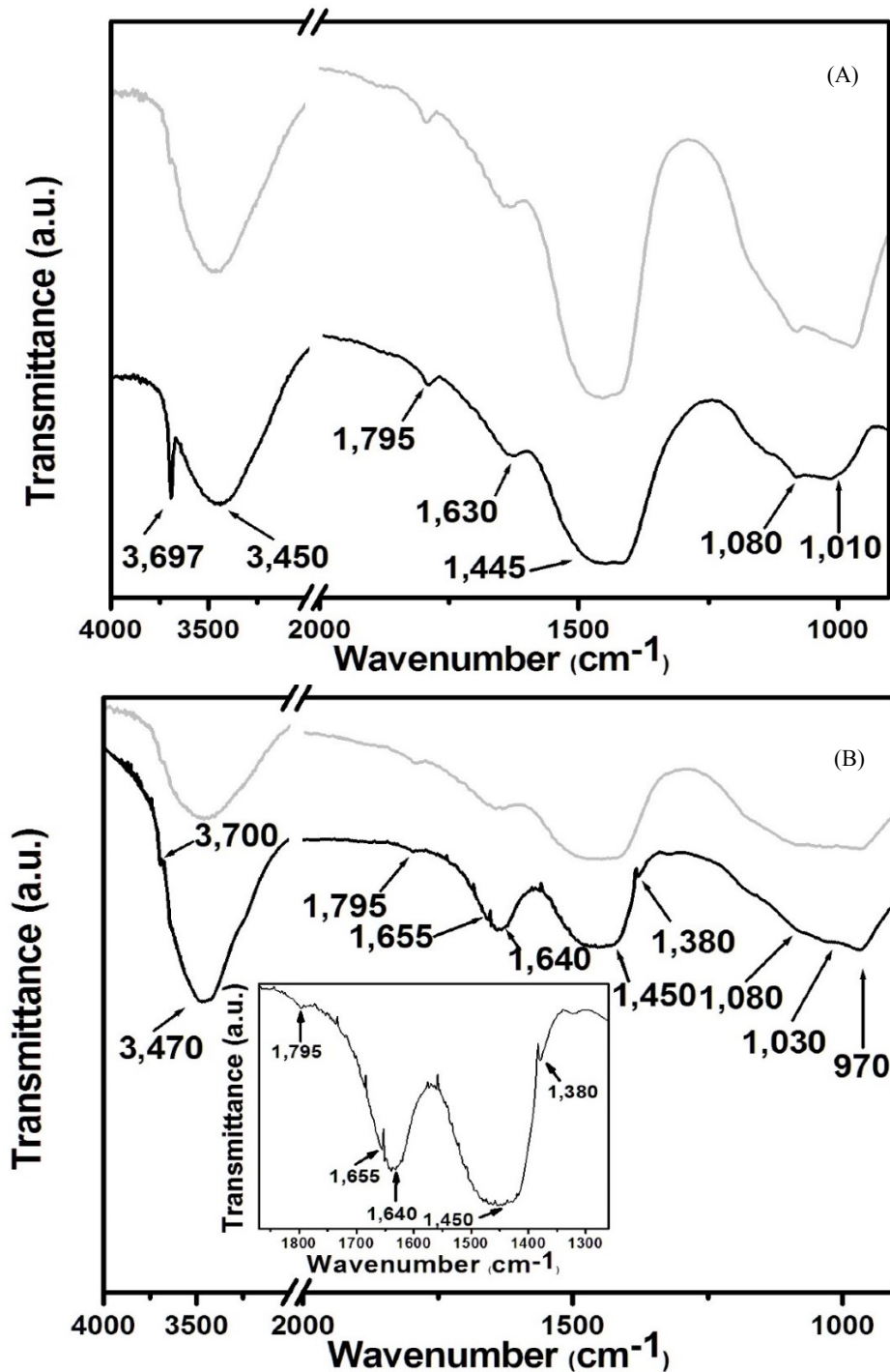


Figure 2: FTIR spectra of slurry-standard (A) and slurry-pol (B). The insert figure in (B) is a magnified view of the bands about 1870 and 1260 cm⁻¹. Black lines: before produced water contact; grey lines: after produced water contact.

Polymers identification within cement-based matrixes is a challenging task, due to the low amounts of such components in cement-based samples. The bands associated with the polymers themselves are difficult to be detected, overlapping with bands of cement phases [24]. However, even the presence of low amounts of water-soluble polymers can influence the properties of the cement-based materials, and a polymer film formation takes place during cement hydration [25]. Anyway, for the FTIR spectrum of slurry-pol, the small bands at 1,380 and 1,655 cm⁻¹ have been attributed to the bending vibration of CH₂ and CH₃ groups and stretching of C=O groups, respectively, all from the structures of the polymers in such slurry [26]. The main difference of the FTIR spectrum of slurry-pol in relation to slurry-standard one is concerned to the absence of CH band at about 3,700 cm⁻¹, even before contact with produced water, suggesting a partial inhibitive effect

of the additives on the formation of CH in slurry-pol.

The X-ray diffractograms of the slurries are presented in Figure 3 and 4. For slurry-standard, the main crystalline products are CH ($2\theta = 18.3$ and 34.3°), poorly crystallized C-S-H ($2\theta = 26.8^\circ$) and ettringite ($\text{Ca}_6\text{Al}_2(\text{SO}_4)_3(\text{OH})_{12}\cdot 26\text{H}_2\text{O}$, $2\theta = 50.3^\circ$), as well as mixtures of quartz and CaCO_3 ($2\theta = 42.5 - 58^\circ$). There are also the presence of unreacted components of cement slurry, such as silica ($2\theta = 21.3^\circ$), C_3S ($2\theta = 29.4$ and 32.4°), C_2S ($2\theta = 39.6^\circ$), C_3A ($2\theta = 47.3^\circ$) and C_4AF ($2\theta = 36.7^\circ$) [27]. The peaks of belite are frequently overlapped by ones of alite, which tends to difficult the analysis of many crystalline phases of cement samples. It is also difficult to rule out the presence of CaCO_3 phases in the diffractograms of the samples, because most of carbonate-related peaks overlap peaks of unreacted alite and belite [28].

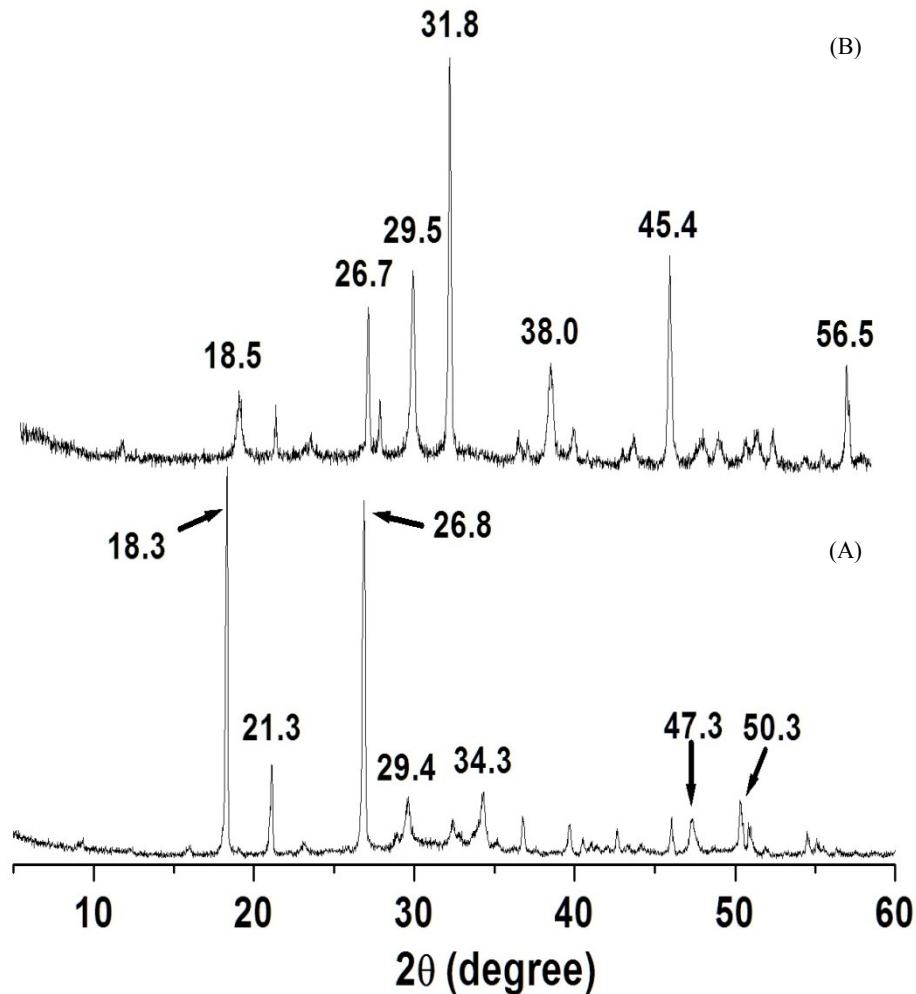


Figure 3: X-rays diffractograms of slurry-standard, before (A) and after (B) contact with produced water.

For slurry-pol, a relatively similar diffractogram profile can be observed. The peak of CH at $2\theta = 18^\circ$ markedly decreased in intensity in relation to slurry-standard diffractogram, which is also consistent with the inhibitive effect of the additives of slurry-pol, as previously suggested by comparative FTIR spectra of the slurries. On the other hand, the high intensity of this diffraction peak is not necessarily related to a high concentration of crystalline CH, rather to CH crystals growth in specific directions [29]. Literature reports that some organic-type additives interact chemically with cement hydration products and may induce irregular crystalline formation of CH and C-S-H [29].

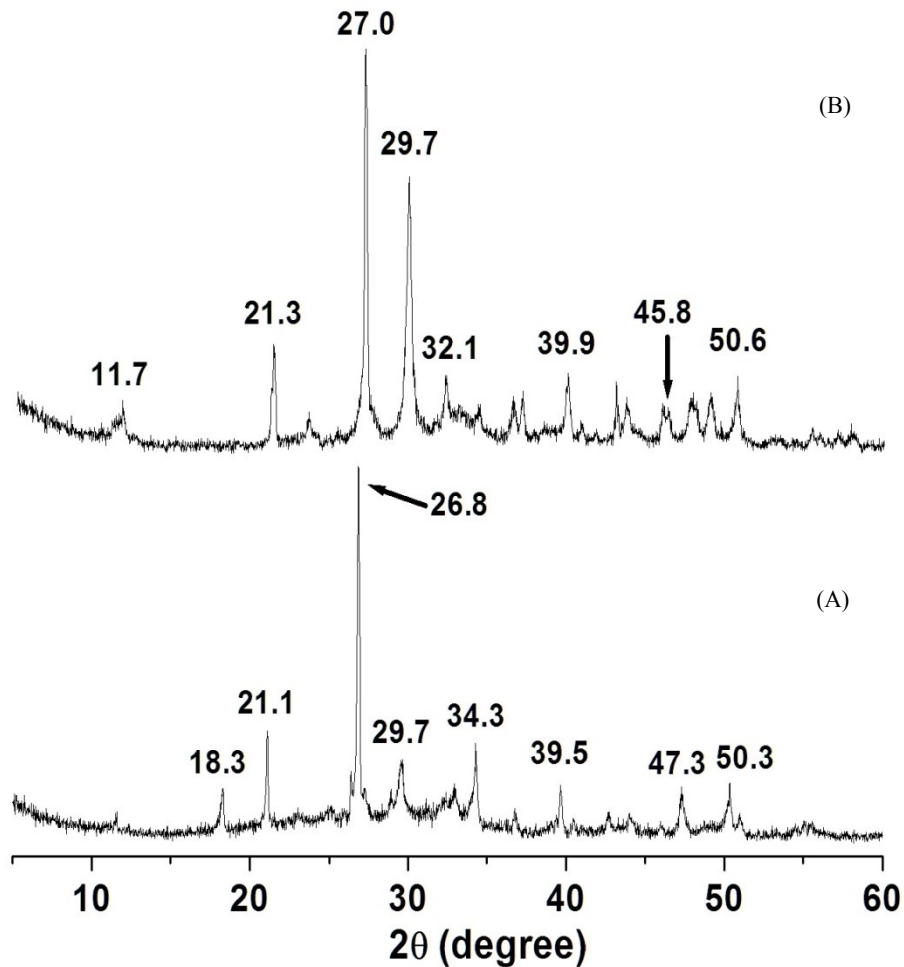


Figure 4: X-rays diffractograms of slurry-pol, before (A) and after (B) contact with produced water.

After long-term contact with produced water, additional crystalline products were detected in the diffractograms of both cement slurries: NaCl ($2\theta = 29.5$ and 45.4°), CaCl_2 ($2\theta = 38^\circ$), Friedel's salt ($[\text{Ca}_4\text{Al}_2(\text{Cl})_2(\text{OH})_{12} \cdot 10\text{H}_2\text{O}]$, $2\theta = 11.2^\circ$) and Kuzel's salt ($[\text{Ca}_2\text{Al}(\text{OH})_6] \cdot [\text{Cl}_{0.50}(\text{SO}_4)_{0.25} \cdot 2.5 \text{H}_2\text{O}]$, $2\theta = 31.8^\circ$). The observed depletion of almost all CH has been attributed to washing out/leaching by the produced water, but some CH might also be consumed by possible formation of brucite $[\text{Mg}(\text{OH})_2]$, calcium carbonate and ettringite, mainly close to the exposed surface of the specimens [30].

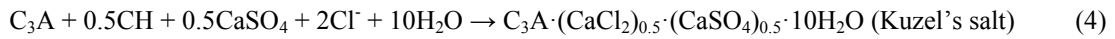
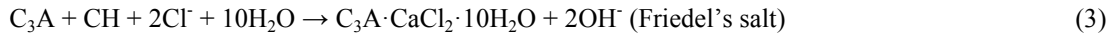
Kuzel's salt is composed of a positively charged layer of $[\text{Ca}_2\text{Al}(\text{OH})_6]^+$ cations and a negatively charged interlayer, with the presence of Cl^- and SO_4^{2-} anions. In this work, the formation of Kuzel's salt on the cement samples is likely to be related to the presence of Cl^- and SO_4^{2-} ions in the produced water. However, it can be noted that Kuzel's salt was only detected in slurry-standard ($2\theta = 31.8^\circ$) and the reason for this is unknown to the authors. The hydrated cement slurries exposed may also induce reaction between NaCl, CaCl_2 and CH with C_3A , producing both Friedel's and Kuzel's salts [31].

From inspection of Figure 3 and 4, additional ettringite is found only in the diffractogram of slurry-standard ($2\theta = 38^\circ$). Crystals of ettringite have been described as columns of $\text{Ca}_3[\text{Si}(\text{OH})_6 \cdot 12\text{H}_2\text{O}]^{3+}$ cations with channels contain the SO_4^{2-} anions and H_2O . The SO_4^{2-} in the produced water could form gypsum (CaSO_4) with additional CH (Equation 1), and the gypsum will lead to ettringite formation (Equation 2) [23, 32].



Additionally, it is relatively well accepted that ettringite formation can promote the ingress of Cl^- ions

in hardened cement bodies. According to current understanding, the presence of Cl^- from ettringite in a particular cement slurry may lead to an increase in the solid volume, which might lead to undesirable expansion and cracking of cement specimen [4]. In this work, the presence of SO_4^{2-} from produced water may result in enrichment in ettringite, which can affect Cl^- ingress into the cement specimens. “Free” Cl^- ions can be bound in calcium chloroaluminate hydrates forming Friedel’s salts or Kuzel’s salts in the pore solution, according to the general Equation 3 and 4.



The analysis of the diffractogram of slurry-pol, however, indicates the presence of lower amounts of CH in relation to the slurry-standard one, as well as apparent absence of ettringite, both characteristics contributing to physical stability of this slurry in the presence of high-saline produced water. The absence of such XRD peak at $2\theta = 38^\circ$ seems to be related to the lower amount of CH in slurry-pol. Therefore, there is an apparent direct relation between the presence of CH with formation of Kuzel’s/Friedel’s salts and ettringite [30, 31].

In order to reach specific understanding on the structures of the cement slurries, the crystallite size of some components of the cement slurries was calculated by Scherrer’s equation (Equation 5) [33]. The results are presented in Table 4. Only specific diffraction peaks of CH, NaCl, Friedel’s and Kuzel’s salts were chosen for calculating the respective crystallite sizes, because some important diffractions peaks of these compounds are sharp and relatively isolated from others.

$$L = \frac{0.89\lambda}{B_{hkl} \cos\theta} \quad (5)$$

L is the crystallite size of a given crystalline compound, hkl are the Miller indices of the planes analyzed, λ is the wavelength of the X-rays, B_{hkl} is the width at half-maximum of a given X-ray diffraction peak in radians and θ is the Bragg angle. The average crystallite sizes of all selected crystalline phases for both slurries were smaller when they are present in slurry-pol. Thus, this finding seems to reinforce the findings described earlier in this report that the presence of the additives in slurry-pol partially inhibited the growth of CH, NaCl and Friedel’s/Kuzel’s salts.

Table 4: Crystallite size of some crystalline compounds of slurry-standard and slurry-pol, before and after long-term contact with hyper-saline produced water.

SLURRY-	XRD PHASE (<i>hkl</i>)	CRYSTALLITE SIZE (nm)	
		BEFORE PW CONTACT	AFTER PW CONTACT
standard	CH (001)	50.32	20.77
	NaCl (111)	ND	29.20
	Friedel’s salt (006)	ND	34.87
	Kuzel’s salt (110)	ND	41.49
pol	CH (001)	35.70	ND
	NaCl (111)	ND	20.08
	Friedel’s salt (006)	ND	9.37
	Kuzel’s salt (110)	ND	31.58

PW: Produced Water.

ND: Not detected.

The TG/DTG curves of the slurries are shown in Figure 5 and 6. Thermal analysis has the ability to analyze specific low crystalline cement phases, which do not appear by XRD technique. Since TG curves of slurry-standard and slurry-pol are relatively similar each other in shape, a more accurate analysis of thermal

behavior of the slurries can be made by using the respective DTG profiles. The TG curve of the slurries can be divided into three major parts, representing different kinds of reactions [34].

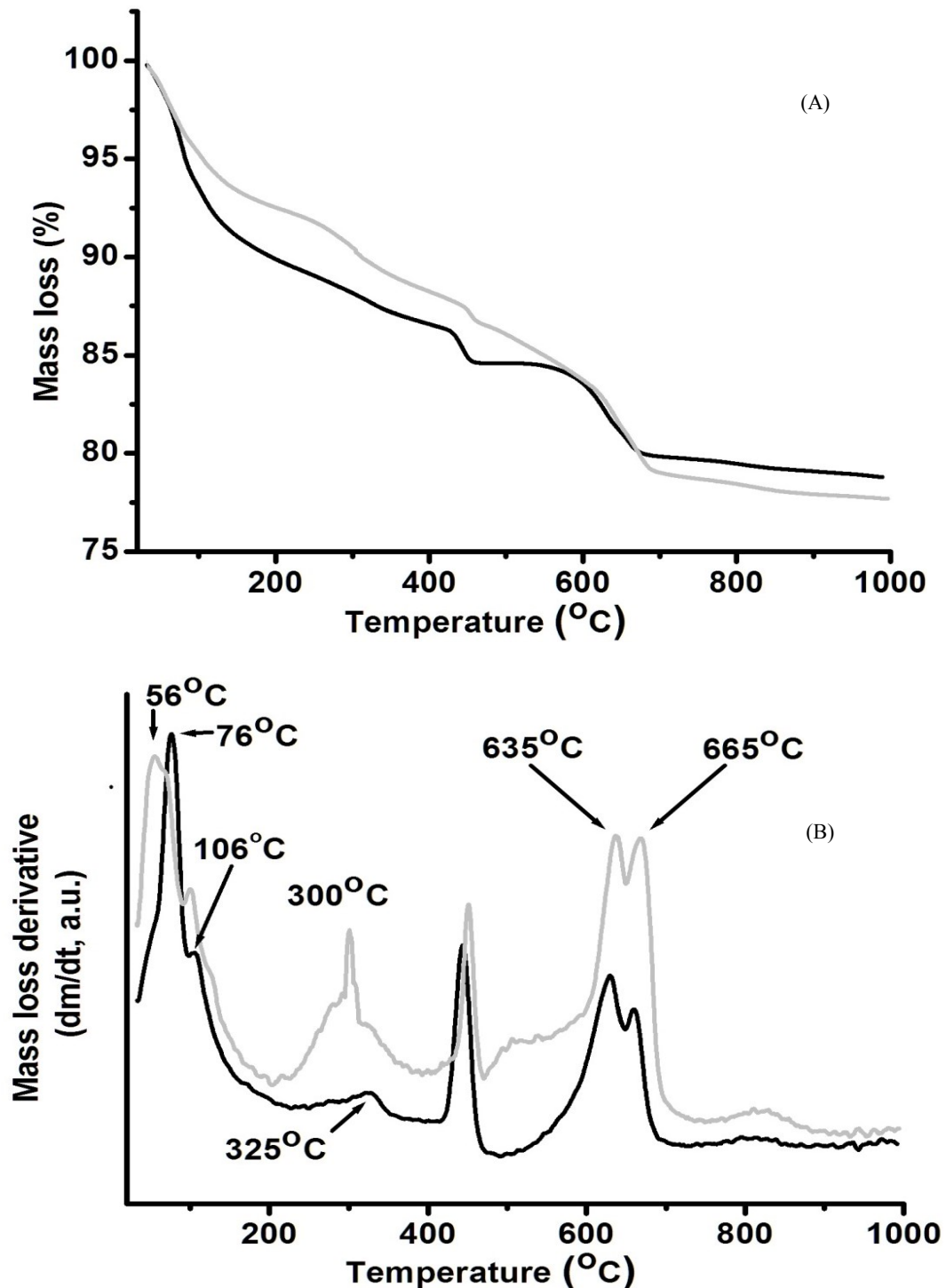


Figure 5: TG (A) and DTG (B) plots of slurry before contact with produce water. Black lines: curves of slurry-standard; grey lines: curves of slurry-pol.

From 25°C up to about 410°C occurred removal of physically adsorbed water from hydrated products, typically C-S-H and ettringite. The range of mass loss in the first part is relatively broad and the corresponding peaks overlap one another during continuous heating processes. Several steps are likely to take place in this area, attributed to loss of capillary pore-, interlayer- and chemically interacted water. Capillary

water is found in capillaries larger than about 50 Å. Interlayer water is the water associated with C–S–H structure by hydrogen bonding. Chemically interacted water is a relatively stable part of the hydration products and removed by high-temperature thermal processes [4].

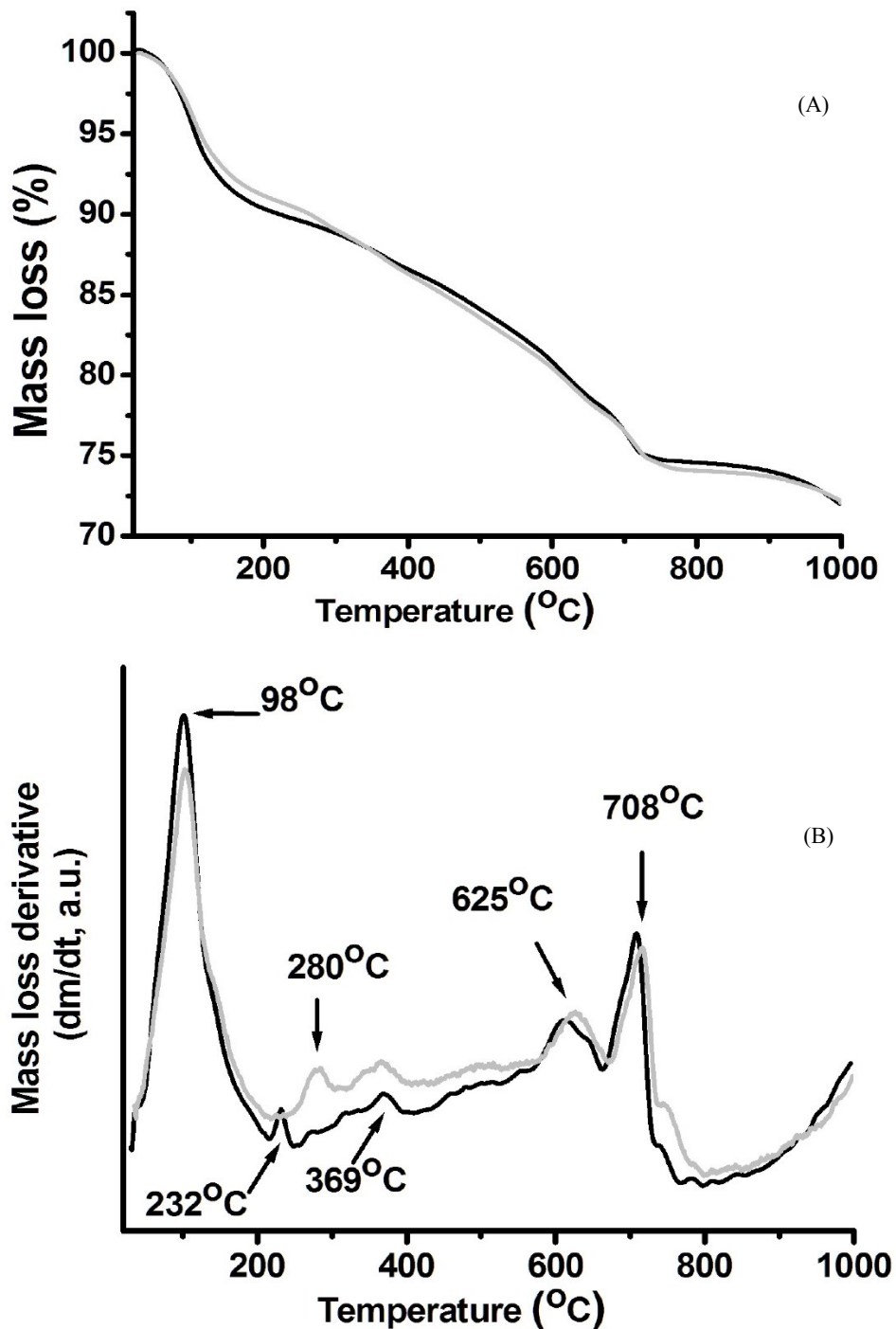


Figure 6: TG (A) and DTG (B) plots of slurry after contact with produce water. Black lines: curves of slurry-standard; grey lines: curves of slurry-pol.

The DTG plot of slurry-standard reveals an initial peak with maximum at 76°C due to loss of physically adsorbed water. For the DTG plot of slurry-pol, the maximum of this peak is shifted to a 56°C. The small peaks in both DTG curves with maxima at ~106°C are due to loss of water of the C–S–H phase. For the DTG curve of slurry-standard, the small broad peak with maximum values of mass loss at 325°C has been assigned to the loss of bound water from decomposition of both C-S-H and carboaluminate hydrates

[34]. For the DTG curve of slurry-pol, the thin peak with maximum at 300°C is most likely in agreement with thermal degradation of the biopolymers CS and ALG.

From 410°C up to about 500°C occurred thermal dehydroxylation of CH. Among the compounds obtained due to cement hydration, CH has been considered of relative precise quantitative determination. The formation of CH determines the overall hydration reaction, as well as influences its mechanical properties of the slurry. The content of CH (%) in all materials was determined using Equation 6, according to the following equation [18, 35]:

$$\text{CH}(\%) = \frac{\Delta_{\text{CH}}(\%) \times M_{\text{CH}}}{M_{\text{W}}} \quad (6)$$

Where $\Delta_{\text{CH}}(\%)$ is the mass loss due to dehydration of CH, M_{CH} is the molar weight of CH and M_{W} is the molar mass of water.

For the slurry-standard and slurry-pol, the CH contents were 7.86 and 5.18%, respectively. After interaction with the produced water, for the slurry-standard, the mass loss related to dehydroxylation of CH is undetectable, but decreased to 1.52% for slurry-pol. It is clear that the addition of the biopolymers and HA reduces the formation of CH, due possibly to absorption of CH on the polymeric films. These results suggest that CH has different structural characteristics in the cement slurries evaluated in this work.

During the reaction of cement with water, the fresh slurry becomes supersaturated with respect to CH, which precipitates in the bulk of the slurry in layered forms with distorted edge-sharing CaO_6 octahedron and can be exfoliated on different substrates [36]. Intralayer bonding in CH is mainly ionic, where each hydroxyl group is linked to three Ca atoms and surrounded by three other hydroxyl groups from an adjacent layer. CH interlayers interactions are, however, of a weak dispersion-type force, since CH crystals are reported to be unable to overcome specific stresses due to nucleation and grow of some hydrates during hydration. The structures and compositions of CH, as well as hydrated silicate and aluminate species have been shown to depend strongly on the presence of polymers, depending mainly on the brand of polymer and the cement/polymer [37]. Polymer particles and films usually act increasing the interparticle bonding between the different layers and strengthen the microstructure of the cement slurry. In the presence of specific polymeric dispersions, CH becomes capable of withstanding those stresses [36, 37].

From about 500°C up to about 1000°C occurred thermal decomposition of carbonate-like phases. The two DTG peaks with maxima at 635 and 665°C have attributed to the decomposition of carbonate-like phases, mainly CaCO_3 [28]. Carbonation reactions may proceed rapidly in the presence of water because of the presence of water-dissolved CO_2 . A simple description of thermal decomposition reaction for CaCO_3 is as follows:



Typically, temperatures below 60°C enable the formation of calcite, and presence of aragonite occurs at higher temperatures. It is well accepted, however, that part of carbonate-like phases may also be formed during thermal analysis [28]. Carbonates are known in three main forms: vaterite, aragonite and calcite. In general, vaterite transforms to calcite or aragonite in the presence of water. CaCO_3 is indeed several orders of magnitude less soluble than CH but in some circumstances; a layer of calcite can significantly protect CH against carbonation and dissolution [38].

For the DTG plots of both slurries, the peaks with maximum intensities at 810 and 830°C have been associated with a C-S-H gel phase formed upon hydration reactions between cement and silica. The exact amount of carbonated phases in cement bodies, however, cannot be reliably calculated from the TG/DTG data, because some C-S-H-type structures also contribute to measured mass loss within this temperature range [35].

The DSC curves of the cement slurries are presented in Figure 7. For the slurry-standard DSC plot, there are three major peaks. The first two broad endothermic peaks centered at 68 and 122°C are the result of removal of physically adsorbed water and loss of water due to dehydration reactions of both C-S-H and ettringite, respectively. The third peak from 295 to 420°C corresponds to the dehydroxylation of CH. For the DSC curve of slurry-pol, there is a first smaller broad endothermic peak from 25 to 165°C. This suggests that C-S-H and ettringite phases have lower amounts of physically adsorbed- and chemically combined water, as well as the peak due to dehydroxylation of CH. Additionally, it is also important to point out that the

behavior of the baselines of the DSC curves also provides additional information on the thermal stability characteristics of slurry-standard and slurry-pol.

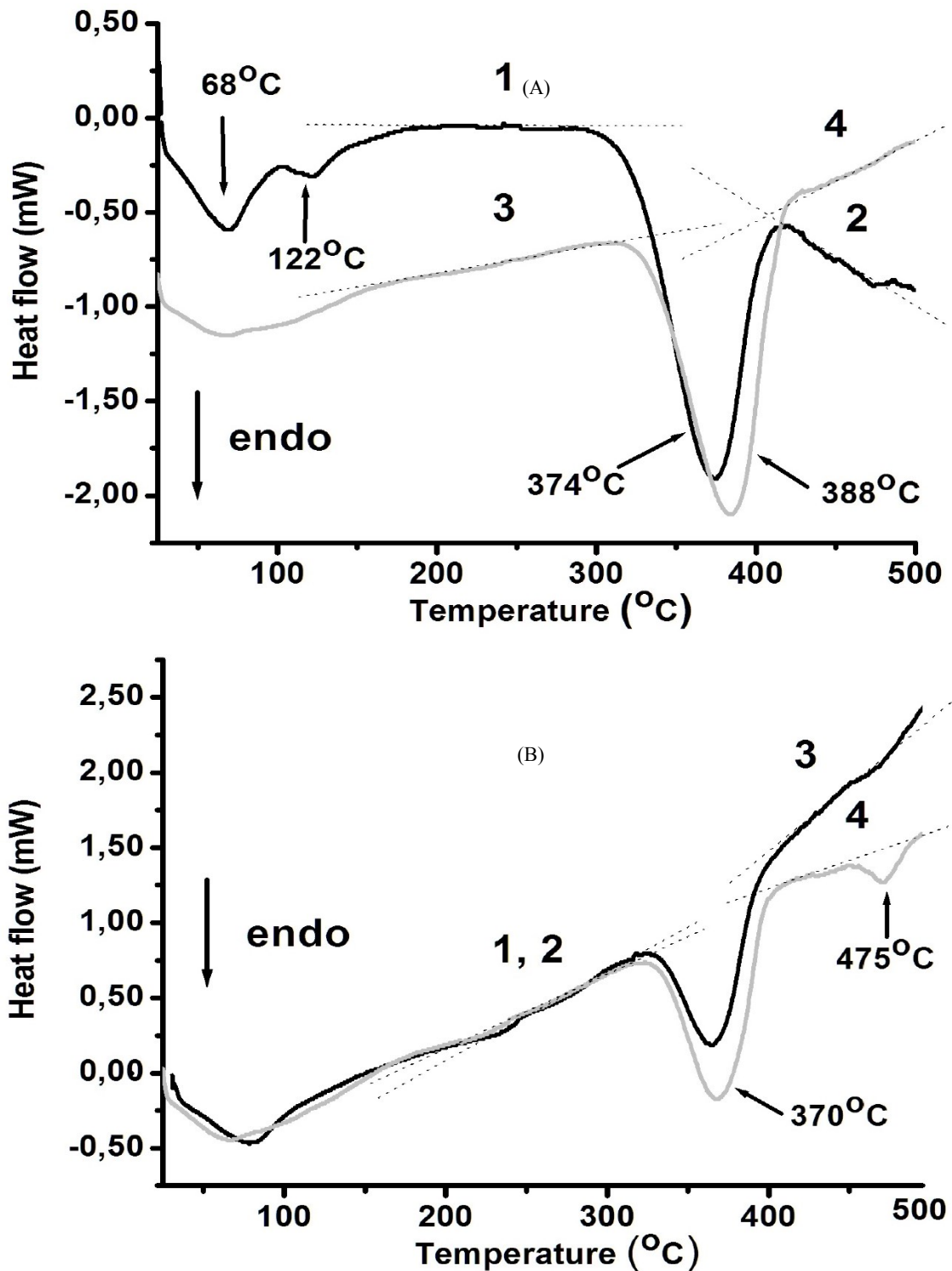


Figure 7: DSC plots of the slurries. Black lines: curves of slurry-standard; grey lines: curves of slurry-pol. (A): before contact with produced water. (B): after contact with produced water. Dashed lines show the behavior of the baseline shifts.

The onset/endset temperatures of CH-related endothermic peaks are 295/420°C (maximum at 374°C) for slurry-standard and 312/430°C (maximum at 388°C) for slurry-pol. It is worthy to point out the DSC

curve of slurry-standard has changed its slope significantly, before and after thermal degradation of CH [sequence 1 → 2 in Figure 7 (A)]. On the other hand, the slope of baseline of the DSC curve of slurry-pol has barely changed, before and after thermal degradation of CH [sequence 3 → 4 in Figure 7 (A)]. For the DSC plots of both slurries after contact with produced water (Figure 7 (B)), the baselines of such plots present the same comparative behavior, for the same sequences 1 → 2 (slurry-standard) and 3 → 4 (slurry-pol). All these findings suggest that slurry-pol has preserved its chemical structure characteristics compared to the slurry-standard ones, even at high temperatures [39, 40].

4. CONCLUSIONS

The presence of the biopolymers and HA has driven the improved self-healing properties observed in the new cement slurry. An important aspect to point out is related to the presence of lower amounts of small crystallite-sized CH in the new cement slurry, in relation to the CH characteristics of standard slurry. Important structural changes have observed for the C-S-H structure of the new slurry, which has presented improved thermal stability characteristics in relation to C-S-H of standard slurry. Significantly, unlike standard slurry, the new slurry has practically maintained its original chemical structure, as well as has shown crystallite-type particles of NaCl and Friedel's/Kuzel's salts with lower dimensions, after long-term contact with produced water from Brazilian oil well fields operations. Because large-size crystalline CH, NaCl and Friedel's/Kuzel's salts are well reported to be weak crystalline phases in most cement-based matrixes, the identification of such slurries components with small crystallite sizes drives the improvement of the self-healing characteristics observed in the new cement slurry.

Further research is needed, evidently, to apply the new slurry for routine oil well cementing operations, from insights gained into characterization. However, the new cement slurry has shown potential to provide improvements in cost effective and environmental-friendly oil well operations.

5. ACKNOWLEDGMENTS

The authors would like to acknowledge Schumberger Petroleum Services (Nossa Senhora do Socorro/SE, Brazil) for the continuous technical support and the Brazilian research agencies National Counsel of Technological and Scientific Development (CNPq) and Higher Education Personnel Improvement Coordination (CAPES) for the financial support to our research group in Brazil and fellowships to I.M.G.S.

6. BIBLIOGRAPHY

- [1] RODRIGUES, L.A., SAUER, I.L., "Exploratory assessment of the economic gains of a pre-salt oil field in Brazil", *Energy Policy*, v. 87, pp. 486-495, Dec. 2015.
- [2] THOMPSON, D.L., STILWELL, J.D., HALL, M., "Lacustrine carbonate reservoirs from Early Cretaceous rift lakes of western Gondwana: Pre-Salt coquinas of Brazil and West Africa", *Gondwana Research*, v. 28, n. 1, pp. 26-51, Aug. 2015.
- [3] BAI, M., SUN, J., SONG, K., *et al.*, "Evaluation of mechanical well integrity during CO₂ underground storage", *Environmental Earth Sciences*, v. 73, n. 11, pp. 6815-6825, June 2015.
- [4] HEWLETT, P.C., *Lea's Chemistry of Cement and Concrete*, Oxford, Elsevier Butterworth Heinemann, 1998.
- [5] LEE, K., NEFF, J., *Produced Water - Environmental Risks and Advances in Mitigation Technologies*, New York, SpringerLink, 2011.
- [6] GREGORY, K., MOHAN, A.M., "Current perspective on produced water management challenges during hydraulic fracturing for oil and gas recovery", *Environmental Chemistry*, v. 12, n. 3, pp. 261-266, May 2015.
- [7] JANSEN, D., GOETZ-NEUNHOEFFER, F., NEUBAUER, J., *et al.*, "Effect of polymers on cement hydration: A case study using substituted PDADMA", *Cement and Concrete Composites*, v. 35, n. 1, pp. 71-77, Jan. 2013.
- [8] HILLOULIN, B., VAN TITTELBOOM, K., GRUYAERT, E., *et al.*, "Design of polymeric capsules for self-healing concrete", *Cement and Concrete Composites*, v. 55, pp. 298-307, Jan. 2015.
- [9] WU, M., JOHANNESSON, B., GEIKER, M., "A review: Self-healing in cementitious materials and engineered cementitious composite as a self-healing material", *Construction and Building Materials*, v. 28, n. 1, pp. 571-583, Mar. 2012.
- [10] WAN NGAH, W.S., TEONG, L.C., HANAFIAH, M.A.K.M., "Adsorption of dyes and heavy metal ions by chitosan composites: A review", *Carbohydrate Polymers*, v. 83, n. 4, pp. 1446-1456, Feb. 2011.

- [11] ZIA, K.M., ZIA, F., ZUBER, M., *et al.*, “Alginate based polyurethanes: A review of recent advances, perspective”, *International Journal of Biological Macromolecules*, v. 79, pp. 377-387, Aug. 2015.
- [12] HAN, J., ZHOU, Z., YIN, R., *et al.*, “Alginate-chitosan/hydroxyapatite polyelectrolyte complex porous scaffolds: preparation and characterization”, *International Journal of Biological Macromolecules*, v. 46, n. 2, pp. 199-205, Mar. 2010.
- [13] PIGHINELLI, L., KUCHARSKA, M., “Chitosan–hydroxyapatite composites”, *Carbohydrate Polymers*, v. 93, n. 1, pp. 256-262, Mar. 2013.
- [14] KONGSRI, S., JANPRADIT, K., BUAPA, K., *et al.*, “Nanocrystalline hydroxyapatite from fish scale waste: Preparation, characterization and application for selenium adsorption in aqueous solution”, *Chemical Engineering Journal*, v. 215-216, pp. 522-532, Jan. 2013.
- [15] VIEIRA, E.F.S., LIMA, P.F., DOS SANTOS, I.M.G., *et al.*, “The influence of in situ polymerized epoxidized A/F bisphenol-chitosan on characteristics of oilwell cement slurry—Molecular-level analysis and long-term interaction of API fracturing fluid”, *Journal of Applied Polymer Science*, v. 131, n. 22, pp. 41044-41053, Nov. 2014.
- [16] CESTARI, A.R., VIEIRA, E.F.S., ALVES, F.J., *et al.*, “A novel and efficient epoxy/chitosan cement slurry for use in severe acidic environments of oil wells-Structural characterization and kinetic modeling”, *Journal of Hazardous Materials*, v. 213-214, pp. 109-116, Apr. 2012.
- [17] CHOUGNET, A., AUDIBERT, A., MOAN, M., “Linear and non-linear rheological behaviour of cement and silica suspensions. Effect of polymer addition”, *Rheologica Acta*, v. 46, n. 6, pp. 793-802, June 2007.
- [18] DÓREA, H.S., BISPO, J.R.L., ARAGÃO, K.A.S., *et al.*, “Analysis of BTEX, PAHs and metals in the oilfield produced water in the State of Sergipe, Brazil”, *Microchemical Journal*, v. 85, n. 2, pp. 234-238, Apr. 2007.
- [19] PICANÇO, M.S., ANGÉLICA, R.S., BARATA, M.S., “Cimentos Portland aditivados com arenito zeolítico com propriedades pozolânicas”, *Revista Matéria (UFRJ)*, v. 19, n. 2, pp. 68-80, June 2014.
- [20] DE WEERDT, K., JUSTNES, H., “The effect of sea water on the phase assemblage of hydrated cement paste”, *Cement and Concrete Composites*, v. 55, pp. 215-222, Jan. 2015.
- [21] DE WEERDT, K., JUSTNES, H., GEIKER, M.R., “Changes in the phase assemblage of concrete exposed to sea water”, *Cement and Concrete Composites*, v. 47, pp. 53-63, Mar. 2014.
- [22] SÁEZ DEL BOSQUE, I.F., MARTÍNEZ-RAMÍREZ, S., BLANCO-VARELA, M.T., “FTIR study of the effect of temperature and nanosilica on the nano structure of C-S-H gel formed by hydrating tricalcium silicate”, *Construction and Building Materials*, v. 52, pp. 314-323, Feb. 2014.
- [23] GENG, J., EASTERBROOK, D., LI, L.-Y., *et al.*, “The stability of bound chlorides in cement paste with sulfate attack”, *Cement and Concrete Research*, v. 68, pp. 211-222, Feb. 2015.
- [24] SOARES, L.W.O., BRAGA, R.M., FREITAS, J.C.O., *et al.*, “The effect of rice husk ash as pozzolan in addition to cement Portland class G for oil well cementing”, *Journal of Petroleum Science and Engineering*, v. 131, pp. 80-85, July 2015.
- [25] KNAPEN, E., VAN GEMERT, D., “Cement hydration and microstructure formation in the presence of water-soluble polymers”, *Cement and Concrete Research*, v. 39, n. 1, pp. 6-13, Jan. 2009.
- [26] LU, Y.-S., LIN, Y.-C., KUO, S.-W., “Separated Coil and Chain Aggregation Behaviors on the Miscibility and Helical Peptide Secondary Structure of Poly (tyrosine) with Poly (4-vinylpyridine)”, *Macromolecules*, v. 45, n. 16, pp. 6547-6556, Aug. 2012.
- [27] DJOUANI, F., CONNAN, C., CHEHIMI, M.M., *et al.*, “Interfacial chemistry of epoxy adhesives on hydrated cement paste”, *Surface and Interface Analysis*, v. 40, n. 3-4, pp. 146-150, Feb. 2008.
- [28] LOTHENBACH, B., LE SAOUT, G., GALLUCCI, E., *et al.*, “Influence of limestone on the hydration of Portland cements”, *Cement and Concrete Research*, v. 38, n. 6, pp. 848-860, June 2008.
- [29] PEREZ, G., GAITERO, J.J., ERKIZIA, E., *et al.*, “Characterization of cement pastes with innovative self-healing system based in epoxy-amine adhesive”, *Cement and Concrete Composites*, v. 60, pp. 55-64, July 2015.
- [30] JONES, M.R., MACPHEE, D.E., CHUDEK, J.A., *et al.*, “Studies using ²⁷Al MAS NMR of AFm and AFt phases and the formation of Friedel’s salt”, *Cement and Concrete Research*, v. 33, n. 2, pp. 177-182, Feb. 2003.
- [31] JENSEN, M.M., DE WEERDT, K., JOHANNESSON, B., *et al.*, “Use of a multi-species reactive transport model to simulate chloride ingress in mortar exposed to NaCl solution or sea-water”,

Computational Materials Science, v. 105, pp. 75-82, July 2015.

- [32] PELISSER, F., GLEIZE, P.J.P., PETERSON, M., "Synthesis of calcium silicate hydrate/polymer complexes", *Revista Ibracon de Estruturas e Materiais*, v. 4, n. 5, pp. 695-701, Dec. 2011.
- [33] YUE, L., SHUGUANG, H., "The microstructure of the interfacial transition zone between steel and cement paste", *Cement and Concrete Research*, v. 31, n. 3, pp. 385-388, Mar. 2001.
- [34] COSTA, E.B., MANCIO, M., TAKIMI, A.S., *et al.*, "Avaliação da perda de massa de farinhas precursoras de clínquer CSAB compostas com lodo de anodização do alumínio", *Revista Matéria (UFRJ)*, v. 19, n. 3, pp. 291-300, Sept. 2014.
- [35] ESTEVES, L.P., "On the hydration of water-entrained cement-silica systems: Combined SEM, XRD and thermal analysis in cement pastes", *Thermochimica Acta*, v. 518, n. 1-2, pp. 27-35, May 2011.
- [36] AIERKEN, Y., SAHIN, H., IYIKANAT, F., *et al.*, "Portlandite crystal: Bulk, bilayer, and monolayer structures", *Physical Review B*, v. 91, n. 24, pp. 245-413, June 2015.
- [37] MOLLAH, M.Y.A., ADAMS, W.J., SCHENNACH, R., *et al.*, "A review of cement-superplasticizer interactions and their models", *Advances in Cement Research*, v. 12, n. 4, pp. 153-161, Oct. 2000.
- [38] RUIZ-AGUDO, E., KUDŁACZ, K., PUTNIS, C.V., *et al.*, "Dissolution and Carbonation of Portlandite [Ca(OH)₂] Single Crystals", *Environmental Science & Technology*, v. 47, n. 19, pp. 11342-11349, Aug. 2013.
- [39] SHA, W., O'NEILL, E.A., GUO, Z., "Differential scanning calorimetry study of ordinary Portland cement", *Cement and Concrete Research*, v. 29, n. 9, pp. 1487-1489, Sept. 1999.
- [40] VAIČIUKYNIENE, D., VAITKEVIČIUS, V., KANTAUTAS, A., *et al.*, "Utilization of By-Product Waste Silica in Concrete - Based Materials", *Materials Research*, v. 15, n. 4, pp. 561-567, July 2012.